



The first firn core from Peter I Island – capturing climate variability across the Bellingshausen Sea

Elizabeth R. Thomas¹, Dieter Tetzner¹, Bradley Markle^{2,3}, Joel Pedro^{4,5}, Guisella Gacitúa⁶, Dorothea Elisabeth Moser^{1,7}, and Sarah Jackson⁸

¹Ice Dynamics and Paleoclimate, British Antarctic Survey, High Cross, Madingley Road, Cambridge, CB23 7XT, UK

²Department of Geological Sciences, University of Colorado, Boulder, CO, USA

³Institute of Arctic and Alpine Science, University of Colorado, Boulder, CO, USA

⁴Australian Antarctic Division, Kingston, TAS 7050, Australia

⁵Australian Antarctic Program Partnership, Institute for Marine and Antarctic Studies, University of Tasmania, Hobart, TAS 7004, Australia

⁶National Centre for Climate Research, Danish Meteorological Institute, Copenhagen, Denmark

⁷Department of Earth Sciences, University of Cambridge, Cambridge, CB2 3EQ, UK

⁸Research School of Earth Sciences, Australian National University, Canberra, ACT 2600, Australia

Correspondence: Elizabeth R. Thomas (lith@bas.ac.uk)

Received: 22 May 2023 – Discussion started: 8 June 2023

Revised: 15 August 2024 – Accepted: 21 August 2024 – Published: 12 November 2024

Abstract. Peter I Island is situated in the Bellingshausen Sea, a region that has experienced considerable climate change in recent decades. Warming sea surface temperatures and reduced sea ice cover have been accompanied by warming surface air temperature, increased snowfall, and accelerated mass loss over the adjacent ice sheet. Here we present data from the first firn core drilled on Peter I Island, spanning the period 2001–2017 CE. The stable water isotope data capture regional changes in surface air temperature and precipitation (snow accumulation) at the site, which are highly correlated with the surrounding Amundsen–Bellingshausen seas and the adjacent Antarctic Peninsula ($r > 0.6$, $p < 0.05$). The firn core data, together with the unique in situ data from an automatic weather station, confirm the high skill of the ERA5 reanalysis in capturing daily mean temperature and inter-annual precipitation variability, even over a small sub-Antarctic island. This study demonstrates the suitability of Peter I Island for future deep-ice-core drilling, with the potential to provide a valuable archive to explore ice–ocean–atmosphere interactions over decadal to centennial timescales for this dynamic region.

1 Introduction

The sub-Antarctic island of Peter I (Peter I Øy) is a former shield volcano (154 km²) that is almost completely covered by a heavily crevassed ice cap. The island's location in the Bellingshausen Sea (68°51'05" S, 90° 30'35" W; Fig. 1) and just 450 km from the coast of West Antarctica makes it a scientifically important site for paleoclimate, ice sheet, and oceanographic studies. The island is situated within the seasonal sea ice zone in a region of the Southern Ocean that has experienced a rapid decline in sea ice cover in recent decades, reaching a record low in February 2023 (Purich and Doddridge, 2023). The rate of sea ice decline in the Bellingshausen Sea since 1979 is comparable to the rate of ice loss in the Arctic (Parkinson, 2019). Reconstructions from ice cores suggest this recent change is part of a 20th century decline, evident in both proxy- and observation-based reconstructions (Abram et al., 2010; Porter et al., 2016; Thomas et al., 2019).

The closest landmass is the Antarctic Peninsula (AP) and Ellsworth Land coast, a region that experienced considerable climate and glaciological change during the 20th century. Surface air temperatures on the AP, recorded at coastal research stations, have increased by as much as 2.5 °C since the 1950s (Turner et al., 2005), constituting the largest warm-

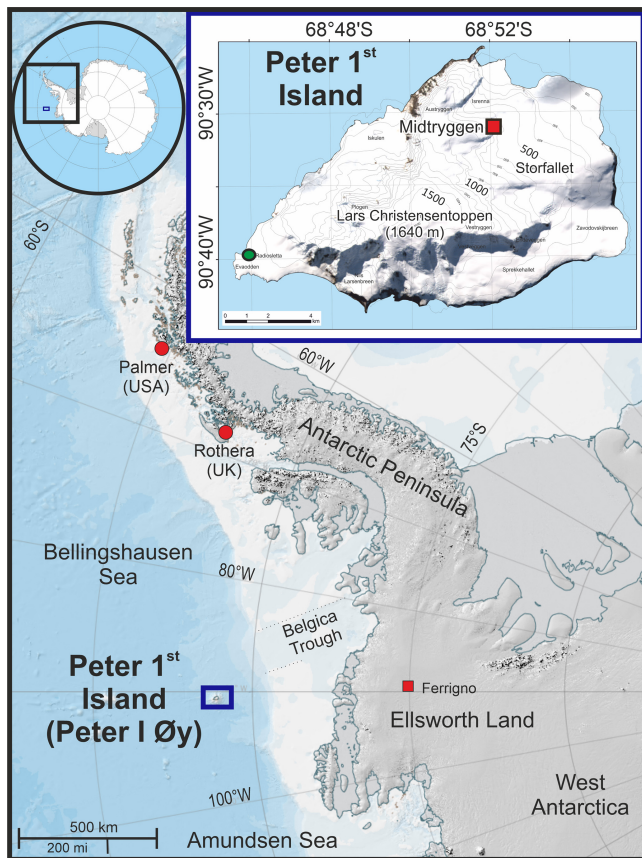


Figure 1. Location of Peter I Island (Peter I Øy) in the Bellingshausen Sea, with the ice core site (blue rectangle), closest Antarctic Peninsula research stations (red circles), and the Ellsworth Land ice core location referenced in the text (Ferrigno, red box) all indicated. The insert map shows the Peter I drilling location (red box), AWS (green dot), and island topography. The map was produced using the Antarctic Digital Database using data made available under the Creative Commons Attribution 4.0 International (CC BY 4.0) licence.

ing in the Southern Hemisphere (Siegert et al., 2019). Despite a pause in the warming trend during the 21st century (Turner et al., 2016), temperatures have continued to increase (González-Herrero et al., 2022), and paleoclimate archives suggest the warming trend during the late 20th century was part of a 100-year trend (Royles et al., 2013; Thomas et al., 2009; Thomas and Tetzner, 2018) that is likely to continue in the future (Li et al., 2018). In addition to the rise in temperature, snowfall increased dramatically during the 20th century (Thomas et al., 2015, 2008, 2017), and this is attributed to changes in atmospheric circulation, sea ice changes, and rising surface air temperature (Goodwin et al., 2016; Medley and Thomas, 2019; Porter et al., 2016).

Glaciers along the Bellingshausen Sea and Ellsworth Land coast have retreated in recent decades (Paolo et al., 2015; Pritchard et al., 2009; Smith et al., 2020). Many glaciers display dynamic thinning and grounding line retreat that

have been attributed to incursions of circumpolar deep water (CDW). The water in the Bellingshausen Sea is amongst the warmest in the Southern Ocean, with measured CDW temperatures exceeding 1°C (Jenkins and Jacobs, 2008). The island is situated to the northwest of the Belgica Fan, the culmination of the Belgica Trough, an exceptionally large paleo-ice stream (Ó Cofaigh et al., 2005). Ice sheet reconstructions suggest that during the Last Glacial Maximum all the modern drainage basins along the Bellingshausen Sea coast were tributaries for a single large ice stream that may have extended to the continental shelf, less than ~ 200 km from Peter I Island. Thus, the location of Peter I Island, at the northern edge of the continental shelf, is of significance for both modern and paleoclimate oceanographic and ice sheet studies.

The first firn core from Peter I Island was drilled as part of the Sub-Antarctic Ice Core Expedition (SubICE), one of the projects of the international Antarctic Circumnavigation Expedition (ACE) 2017–2018 (Thomas et al., 2021). The aim of this study is to present the chemical and stable water isotope data from the Peter I Island ice core to explore its suitability for paleoclimate reconstructions. In addition, we utilize a short instrumental record from an automatic weather station (AWS) from Peter I Island to test the skill of the fifth generation of ECMWF reanalysis (ERA5). ERA5 reanalysis provides hourly data at 0.25° resolution (~ 31 km) with consistent near-surface temperature when compared with observations across Antarctica (Zhu et al., 2021). While the resolution of ERA5 may not fully capture local climate and precipitation on Peter I Island, the AWS and firn core provide a unique opportunity to evaluate the skill of ERA5 at this site. We will (1) establish the firn core age scale, (2) evaluate the skill of ERA5 at this island, (3) evaluate the firn core proxies against meteorological parameters from ERA5, and (4) discuss the suitability of this site for future deep-ice-core drilling.

2 Data and methods

2.1 Ice core site

In February 2017 a shallow ice core was drilled to a depth of 12.29 m on Peter I Island ($68^{\circ} 51'05''$ S, $90^{\circ}30'35''$ W). A site had been selected based on satellite imagery at the plateau at the top of the island (Lars Christentoppen); however, heavy cloud cover prevented a helicopter from landing at this site. Instead, a lower-elevation site was found on a ridge (Midtryggen) at 730 m above sea level in a small saddle on the eastern side of the island overlooking the main glacier Storfallet (Fig. 1). The snow surface was relatively smooth at this site (slope of $\sim 5^{\circ}$), and ground-penetrating radar (GPR) surveys were conducted in a ~ 500 m radius from the drill site (Thomas et al., 2021). Near-continuous stratified layers were observed in the GPR profiles for the upper 43 m at this site (the maximum time window for the GPR), and bedrock

was not detected at this depth; however, the full ice thickness has not been determined.

The firn core was drilled using a motorized Kovacs ice core drill (Mark II) powered by a four-stroke Honda generator, with core retrieval aided by a sidewinder winch. Ice core sections, with a maximum length of 80 cm, were stored in ethylene-vinyl-acetate-treated (EVA) polythene bags in insulated boxes. The ice core boxes were transported via helicopter to a freezer container on the RS *Akademik Tryoshnikov*. The boxes were loaded onto the RRS *James Clark Ross* in Punta Arenas, where they were stored in a dual-compressor freezer unit that was transported directly to the -25°C laboratories at the British Antarctic Survey (BAS). The temperature of the boxes was monitored throughout and remained below -20°C for the duration of the transport. Subsequent subsampling of the cores was undertaken in the -25°C laboratories.

The length and weight of each firn core fragment was measured to calculate density. Based on the measured density profile and the Herron–Langway model, the estimated bubble close-off depth (when the firn air passages become closed at a density of 0.83 kg m^{-3}) is 34.5 m at this site. Visible melt layers $> 1\text{ mm}$ thick were recorded (Thomas et al., 2021), revealing an estimated 11 % of the ice core is affected by melt, comparable to other sub-Antarctic and coastal Antarctic ice core sites (Thomas et al., 2021) but considerably less than the Young Island ice core (Moser et al., 2021). Discrete samples were cut at 5 cm resolution for ion chromatography (IC) and stable water isotope analysis and sealed in Tritan copolymer jars.

2.2 Meteorological data

Meteorological data come from the European Centre for Medium-Range Weather Forecasts (ECMWF) ERA5 analysis (1979–2017) (Hersbach et al., 2020), the fifth generation of ECMWF reanalysis. ERA5 reanalysis currently extends back to 1950, providing hourly data at 0.25° resolution ($\sim 31\text{ km}$). However, we note that the resolution of ERA5 may not fully capture local climate and precipitation on Peter I Island. An AWS was located on the island between February 2006 and January 2007 (<http://amrc.ssec.wisc.edu/aws/index.php?region=OceanIslands&station=PeterI&year=2006>, last access: 3 November 2020). The AWS data provide a short (but incomplete) in situ record of surface temperature (Thomas et al., 2021) covering 149 d between 19 February 2006 and 31 December 2006. These data were not assimilated into the ECMWF model. The AWS was located near $68^{\circ}46.2\text{ S}$, $90^{\circ}30.3\text{ W}$, at a height of $\sim 128\text{ m}$ on the “Radiosletta” Plateau on the NW side of the island (Fig. 1, insert map). Statistical significance values (p) are applied throughout the text using a two-tailed t test.

2.3 Stable water isotopes

Isotopes, $\delta^{18}\text{O}$ and δD , were measured using a Picarro L2130-i analyser at the British Antarctic Survey (BAS) with an accuracy of 0.3 ‰ and 0.9 ‰ , respectively. The measurements are reported against the international standard of Vienna Standard Mean Ocean Water (V-SMOW). Deuterium excess (D_{xs}) is the second-order parameter calculated from the two water isotope ratios ($D_{\text{xs}} = \delta\text{D} - 8 \cdot \delta^{18}\text{O}$).

2.4 Major ion chemistry

Major ion concentrations were measured using a high-performance Dionex Integrion ion chromatograph with an injection volume of $250\text{ }\mu\text{L}$ in a class-100 clean room at BAS. For the cation chromatograph, we applied a guard column type CS16-4 μm ($2 \times 50\text{ mm}$) and a CS16-4 μm separator column ($2 \times 250\text{ mm}$). For the anion chromatograph, we used an AG17-C guard column ($2 \times 50\text{ mm}$) together with an AS17-C analytical column ($2 \times 250\text{ mm}$). The chemical data presented here are for the purposes of annual-layer counting. Ions include sulfate [SO_4^{2-}], methanesulfonic acid [MSA^-], bromide [Br^-], and sodium [Na^+], with an analytical precision defined as the relative standard deviation of the lowest level standard of 0.03, 0.07, 0.003, and 0.07 ppb, respectively.

2.5 Microparticles

Ice samples were filtered through 13 mm diameter, $1.0\text{ }\mu\text{m}$ pore size WhatmanTM polycarbonate membrane filters inside clean polypropylene SwinnexTM filter holders. Filters were mounted onto aluminium stubs for analyses on a scanning electron microscope (SEM) at the Earth Sciences Department of the University of Cambridge. Filters were imaged on a Quanta-650F using backscattered electrons in a low-pressure mode. Each filter was imaged at $800\times$ magnification for cryptotephra identification and physical characterization, following the analysis strategy presented in Tetzner et al. (2021).

2.6 Snow accumulation

The annual snow accumulation is derived from the annual-layer thickness (see Sect. 3.1). The thickness is converted to metres of water equivalent (m w.e. yr^{-1}) based on the measured density. Thinning is corrected using the Nye model, which assumes thinning is proportional to vertical stress, appropriate for the upper 10 % of the ice sheet (Nye, 1963). While the ice cap thickness is unknown at this site, GPR confirms that bedrock is at least deeper than 43 m (Thomas et al., 2021). Given the site’s elevation (730 m a.s.l) and the relatively flat surface topography, a depth of 130 m is not unreasonable. While we assume that the 14 m firn core is likely within the upper 10 % of the ice cap, and thus suitable for the Nye model (Nye, 1963), we acknowledge that this might not be the most appropriate thinning function for this site.

3 Results

3.1 Age scale

The age scale has been derived using annual-layer counting based on the $\delta^{18}\text{O}$, D_{xs} , and seasonal deposition of major ion chemistry (Fig. 2). Clear seasonal cycles are observed for D_{xs} observed at sites in the northern Antarctic Peninsula (Fernandoy et al., 2018). Given its maritime location, seasonal cycles are especially clear in sea salt ions, i.e. $[\text{Na}^+]$ and $[\text{Cl}^-]$, and chemical species with marine origin, including $[\text{SO}_4^{2-}]$ and $[\text{Br}^-]$. These species relate to changes in marine productivity and sea ice (e.g. Thomas et al., 2019, and references therein), which peak during the phytoplankton bloom in spring and summer. Both $[\text{SO}_4^{2-}]$ and $[\text{MSA}^-]$ are robust seasonal markers in many coastal Antarctic ice cores (Emanuelsson et al., 2022; Tetzner et al., 2022; Thomas and Abram, 2016) and have also proved to be valuable for dating other sub-Antarctic ice cores (King et al., 2019; Moser et al., 2021).

Summer peaks were assigned if a consistent peak was observed in the D_{xs} (Fig. 2b) and marine ions (Fig. 2c–f). The $\delta^{18}\text{O}$ record (Fig. 2a) was used as a secondary tracer. An equal number of peaks are identified in the D_{xs} , $\delta^{18}\text{O}$, and ions records; however, there is often an offset in the location of the peak. The location of the peaks is assumed to represent approximately November–December, corresponding to the summer sea ice break-up. The final age scale spans from summer 2017 until summer 2002, encompassing 15 full years.

A prominent peak in major ion chemistry (including $[\text{SO}_4^{2-}]$) at 4.6 m depth corresponds to the Puyehue–Cordón Caulle eruption from southern Chile (Fig. 2). This VEI5-rated eruption began in June 2011 and has been observed in a West Antarctic snow pit during the austral winter of 2011 (Koffman et al., 2017). The peak in our record appears in late 2011 and into 2012 and provides at least one independent reference horizon. High biogenic $[\text{SO}_4^{2-}]$ background can make identification of volcanic $[\text{SO}_4^{2-}]$ peaks difficult, as demonstrated at Antarctic Peninsula sites (Emanuelsson et al., 2022; Tetzner et al., 2021). While the average $[\text{SO}_4^{2-}]$ is lower at Peter I than many coastal Antarctic sites (Thomas et al., 2023), the background $[\text{SO}_4^{2-}]$ may make identification of bipolar eruptions difficult. The lower end of the age scale is characterized by the absence of the recently identified Sturge Island eruption in 2001 (Tetzner et al., 2021). This sub-Antarctic eruption has been detected as large shards at other sub-Antarctic islands (Moser et al., 2021) and the Ellsworth Land coast adjacent to Peter I Island. Although this is not definitive, we might expect to see some evidence of this eruption at this site if our age scale extended beyond 2002.

Microparticle analysis was included to identify potential cryptotephra shards. Distinct shards were observed between 4.6–4.9 m depth, which display sharp edges and a glassy appearance typical of tephra morphology (Fig. 3). The shards

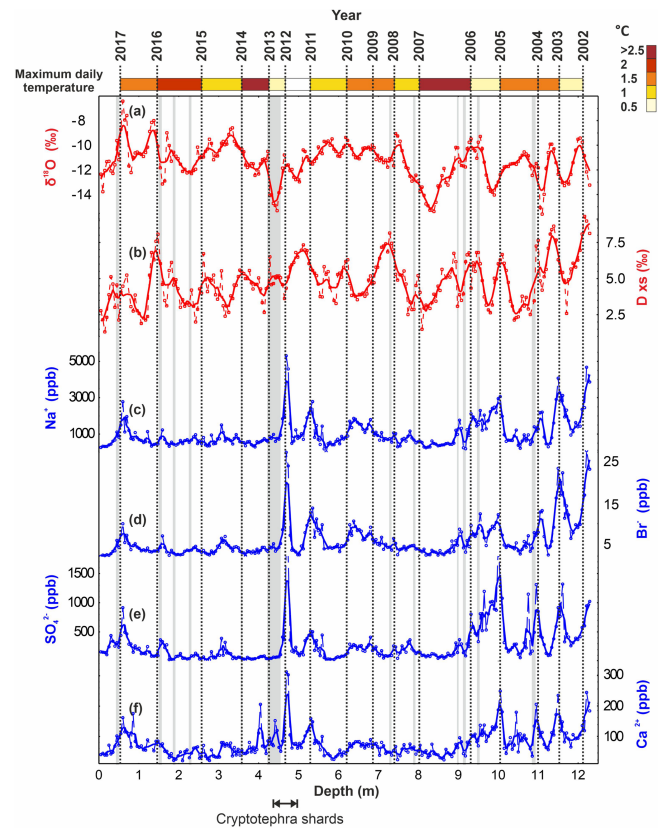


Figure 2. Annual-layer counting based on (a) stable water isotopes ($\delta^{18}\text{O}$), (b) deuterium excess (D_{xs}), (c) sodium $[\text{Na}^+]$, (d) bromide $[\text{Br}^-]$, (e) sulfate $[\text{SO}_4^{2-}]$, and (f) calcium $[\text{Ca}^{2+}]$; all species are plotted at 5 cm resolution (dashed curves) with a three-point running mean (solid curves). Vertical dashed black lines indicate the location of summer peaks (approximately January). Vertical grey shading indicates observed melt layers of greater than 5 cm thickness. The location of cryptotephra shards (Fig. 3) is identified in the layer corresponding to 2011–2012. The top colour bar represents the maximum daily 2 m temperature ($^{\circ}\text{C}$) from ERA5, with calendar years indicated above.

appear in the same layer as the $[\text{SO}_4^{2-}]$ peak, corresponding to dates from approximately austral winter 2011 to austral autumn 2012. This is consistent with observations from West Antarctica (Koffman et al., 2017). The presence of cryptotephra shards corresponding to the Puyehue–Cordón Caulle eruption (2011) and the absence of shards corresponding to the Sturge Island eruption (2001) further support our age scale.

An evaluation of the visible melt layers for this site suggests that 11% of the total ice core is classified as melt (Thomas et al., 2021). This percentage is driven largely by a single 30 cm thick melt layer at a depth of 4.5 m (Fig. 4a). Based on our annual-layer counting, this melt feature corresponds to the year 2012 CE. Over a period of 21 d in January 2013, the daily temperature (ERA5, not corrected for elevation) remained above 0.5°C , reaching a maximum daily

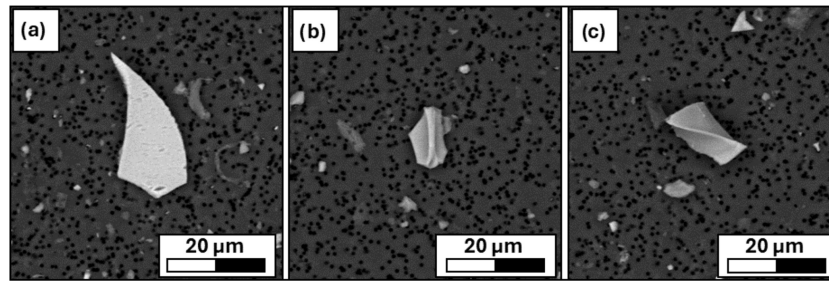


Figure 3. Shards identified from the interval 4.6–4.9 m depth displaying typical cryptotephra morphology. The images were obtained using a Quanta-650F scanning electron microscope (SEM) at the Earth Sciences Department of the University of Cambridge. Each filter was imaged at $\times 800$ magnification using backscattered electron imagery (BSEI) in a low-pressure mode.

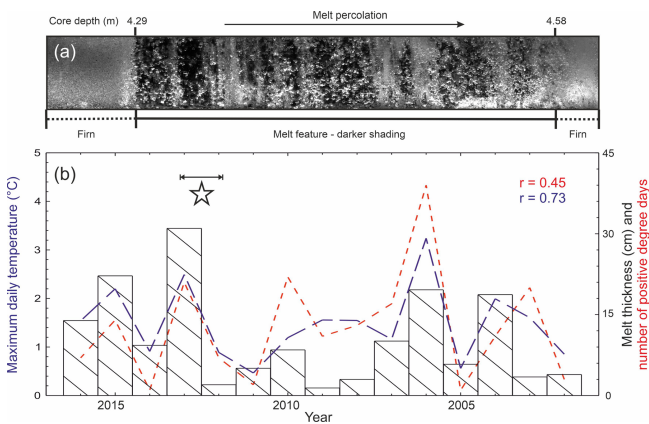


Figure 4. (a) Line-scanned image of the Peter I firn core highlighting the prominent melt feature, observed as a dark area (higher density) between 4.29–4.58 m depth, compared to the lighter-shaded (lower density) areas corresponding to firn. (b) Comparison of the annual melt thickness (black bars, cm) in the firn core with the number of positive degree days (red, temperature $> 0.5\text{ }^{\circ}\text{C}$) and the maximum daily temperature (blue, $^{\circ}\text{C}$) from ERA5. The star highlights the location of the melt feature (a), which is observed in the 2012 layer but assigned to 2013 due to the downward percolation of meltwater generated during January 2013.

temperature of $2.5\text{ }^{\circ}\text{C}$ (Fig. 4b). The prolonged mild conditions in January 2013 likely explain the thick melt feature observed in the year corresponding to 2012 (Fig. 4a). This is a result of the downward percolation of surface meltwater, which has affected the snow accumulated during the previous autumn and winter (e.g. Moser et al., 2024)

The second-most melt-affected year is 2006 CE. A maximum daily temperature of $3.2\text{ }^{\circ}\text{C}$ (ERA5) was recorded in February 2006, the warmest month in the record. Between February and March 2006, maximum daily temperatures exceeded $0.5\text{ }^{\circ}\text{C}$ for a total of 39 d. Positive temperatures during 2006 are corroborated by AWS data, which recorded a maximum daily temperature of $1.94\text{ }^{\circ}\text{C}$. The downward percolation of surface melt is observed in melt features spanning the summer peak corresponding to 2005/2006.

A positive relationship ($r = 0.45$, $p < 0.1$) is observed between positive degree days (ERA5, temperature $> 0.5\text{ }^{\circ}\text{C}$) and annual melt thickness (Fig. 4b). The two warmest years on the record, 2006 and 2013 CE, correspond to the most melt-affected sections in the core (2006 and 2012), with a significant correlation ($r = 0.73$, $p < 0.01$) between maximum daily 2 m temperature and melt thickness. The alignment of the melt features provides further independent verification for the proposed age scale.

3.2 Evaluating the skill of ERA5 reanalysis to capture temperature

The Peter I firn core and the in situ observations from an AWS provide a unique opportunity to evaluate the skill of the latest generation of reanalysis, ERA5, at a remote sub-Antarctic island. The hourly temperature data recorded by the AWS have been converted to daily averages for comparison (Fig. 5a). The AWS recorded intermittently from February to December 2006, and averages were only calculated on days when greater than 50 % of the hourly data were available. There is exceptional agreement between the AWS and ERA5 daily data, with a correlation coefficient of $r = 0.91$ for the days of overlap ($n = 149$, $p < 0.0001$). This demonstrates the high degree of skill in the ERA5 reanalysis data, although the period of comparison is short. The average daily temperature from the AWS data was $-3.09\text{ }^{\circ}\text{C}$, $0.93\text{ }^{\circ}\text{C}$ colder than the same days in ERA5. The correlation coefficient is maintained even when increasing the threshold to only include days when greater than 90 % of the hourly data were available ($r = 0.91$, $n = 105$, $p < 0.0001$). However, when only incorporating data above the 90 % threshold, the temperature difference between ERA5 and AWS increases to $1.07\text{ }^{\circ}\text{C}$.

Due to the adiabatic rate of temperature change in vertically moving air, we would expect slightly colder temperatures at the AWS site (128 m above sea level). A difference of $1.07\text{ }^{\circ}\text{C}$ between the AWS and ERA5 temperatures would suggest a lapse rate of $0.86\text{ }^{\circ}\text{C } 100\text{ m}^{-1}$. This is higher than the lapse rate of $0.68\text{ }^{\circ}\text{C } 100\text{ m}^{-1}$ applied in Thomas et al. (2021) based on the measured rate in the western Antarc-

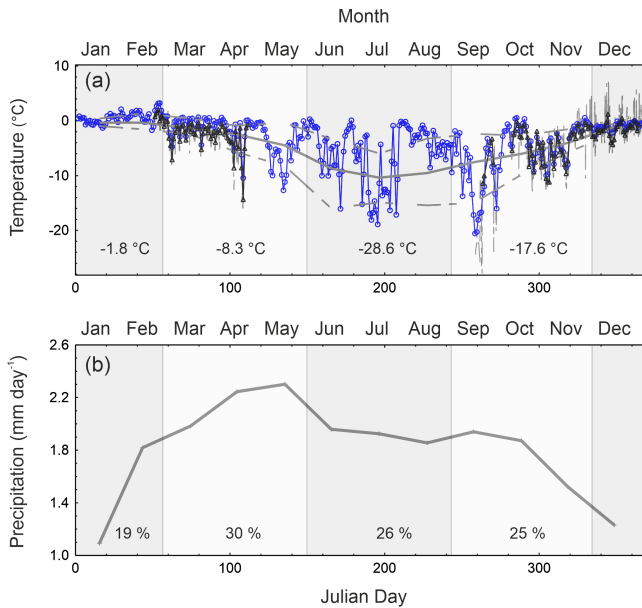


Figure 5. Seasonal cycle in temperature (a) and precipitation (b) at Peter I Island from ERA5 reanalysis (grey curve) (2002–2016 CE). The dashed grey curve represents percentiles 2.5 and 97.5 for temperature (a). Daily average temperatures during 2006 CE from ERA5 (blue circle) and AWS (black triangle), with hourly AWS temperature shown as a thin grey curve. Grey shading highlights the seasons, with the corresponding average temperature and percentage of precipitation shown. AWS data are available from the University of Wisconsin–Madison Automatic Weather Station Program.

tic Peninsula (Martin and Peel, 1978). However, if a lapse rate of 0.86 °C is applied to the ERA5 data, this would suggest that maximum daily temperatures at the drill site did not exceed -2.8 °C in the period 2002–2016. This does not fit the evidence of visible melt features in the firn core.

The appearance of melt features results from a dynamic interplay of atmospheric and snow conditions. However, it is a reasonable assumption that melting will occur when temperatures have exceeded 0 °C , even if only for a few hours. Thus, the discrepancy between ERA5 temperatures and visible melt features in the ice core could suggest that a lower lapse rate is required. To test this discrepancy, we explore the relationship between temperature and melt in the firn core.

If we assume that the melt features corresponding to 2013 (captured in the 2012 layer, Fig. 4a) and 2006 arose due to positive degree days at the drill site, then we can estimate the lower lapse rate threshold. This is based on the maximum daily temperature in ERA5 during 2013 (2.5 °C) and 2006 (3.2 °C) divided by the difference in elevation at the drill site (730 m). This approach produces a lapse rate estimate of $0.34\text{ °C }100\text{ m}^{-1}$ for 2013 and $0.44\text{ °C }100\text{ m}^{-1}$ for 2006. Applying the same approach to the AWS maximum daily temperature (1.94 °C during 2006) produces a slightly lower value of $0.32\text{ °C }100\text{ m}^{-1}$. These estimates are at the lower

end of the moist adiabatic lapse rate ($0.4\text{--}0.6\text{ °C }100\text{ m}^{-1}$) and lower than lapse rates measured at the sub-Antarctic Macquarie Island (Fitzgerald and Kirkpatrick, 2020). However, lapse rates as low as $0.31\text{ °C }100\text{ m}^{-1}$ have been reported at the sub-Antarctic Marion Island (Nyakatya and McGeoch, 2008).

Applying the estimated lapse rate range, $0.32\text{--}0.44\text{ °C }100\text{ m}^{-1}$, reduces the difference between the AWS and ERA5 temperature from 1.07 °C to between $0.67\text{--}0.52\text{ °C}$. This is likely a conservative estimate because 0 °C is the lower limit for melt. However, this suggests that the warmer daily temperatures in ERA5 cannot be explained by differences in elevation alone and may suggest a warm bias in the ERA5 data of between $0.52\text{--}0.67\text{ °C}$ at this location.

3.3 Evaluating the skill of ERA5 reanalysis to capture precipitation

In the absence of daily precipitation data from the AWS, we can use the snow accumulation derived from the firn core to evaluate the skill of ERA5 in capturing inter-annual precipitation variability. The average snow accumulation derived from the firn core (2002–2016) is $0.49\text{ m w.e. yr}^{-1}$. This is slightly lower than the estimated precipitation–evaporation ($P-E$) value of $0.55\text{ m w.e. yr}^{-1}$ from ERA5 for this site (Fig. 5a). Case studies on the AP and coastal Ellsworth Land using the previous generation of reanalysis products (ERA-Interim and ERA-40) suggest that snow accumulation is underestimated by between 0.025 and $0.26\text{ m w.e. yr}^{-1}$ (Thomas and Bracegirdle, 2009, 2015). In this more maritime setting, notwithstanding the different orographic positions of the firn core site on the island, there is an offset of approximately 6 cm yr^{-1} ($\sim 12\%$) between the snow accumulation recorded in the firn core and ERA5 ($P-E$).

Snow accumulation is the sum of precipitation, evaporation, melt, erosion, and sublimation. Wind-driven erosion and redistribution are estimated to remove between $5\text{--}20\text{ cm yr}^{-1}$ of precipitated snow in Antarctic coastal regions (Lenaerts and van den Broeke, 2012), which is within the lower range of our observed offset. In addition, we have already established that this site is influenced by melt, which not only alters the density calculations but may also suggest potential loss as melt run-off.

3.4 Snow accumulation

Snow accumulation (2016–2002) at Peter I Island is positively correlated with $P-E$ from ERA5. Strong correlations are observed over the island ($r=0.75$, $p<0.01$), with an extended zone of correlation ($r>0.6$) across the Bellingshausen Sea, the Antarctic Peninsula, and the Ronne–Filchner Ice Shelf (Fig. 6b).

A positive correlation is also observed between snow accumulation and surface air temperature from ERA5 ($r=0.59$,

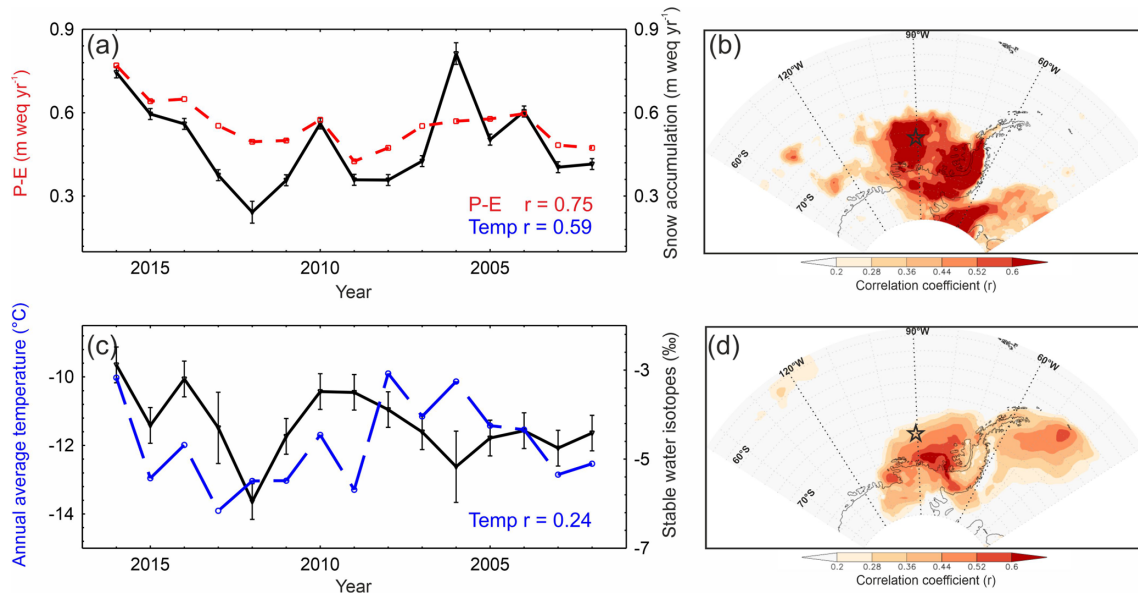


Figure 6. (a) Peter I Island annual-average snow accumulation (solid black) compared with precipitation–evaporation ($P-E$) (dashed blue) from ERA5 reanalysis data (2002–2016). The corresponding correlation coefficients (r) for snow accumulation and $P-E$ (red) and snow accumulation with 2 m temperature (blue) are also shown. (b) Spatial correlation plot of annual snow accumulation with annual ERA5 $P-E$ (all coloured areas $p > 0.05$). (c) Annual-average stable water isotope ($\delta^{18}\text{O}$) (solid black) compared with annual-average 2 m temperatures from ERA5 (dashed blue). The correlation coefficient (r) between annual $\delta^{18}\text{O}$ and annual-average 2 m temperature (blue) is also shown. (d) Spatial correlation plot of annual $\delta^{18}\text{O}$ with annual ERA5 2 m temperature (all coloured areas $p > 0.05$). All annual averages are calculated as December to November. Uncertainty bars are a single standard error (σ) for all years except 2006 and 2012, where 2σ is applied to account for additional uncertainties relating to melt.

$p < 0.05$). The spatial extent of the correlations (not shown) broadly mirrors the relationship with precipitation (Fig. 6b), extending from the Bellingshausen Sea over the Antarctic Peninsula.

3.5 Stable water isotopes

The stable water isotope composition of Antarctic snow-fall has been used to reconstruct past surface temperatures at annual to centennial timescales (e.g. Stenni et al., 2017, and references therein). However, the processes controlling isotopic composition are complex, relating to water vapour origin, distance from source (Hatvani et al., 2017), condensation conditions, fractionation pathways (Markle and Steig, 2022), precipitation seasonality, intermittency, and post-depositional changes (Münch et al., 2017; Fernandoy et al., 2012).

The annual-average stable water isotopes (both $\delta^{18}\text{O}$ and δD) at Peter I Island are weakly correlated with ERA5 2 m temperatures at the site ($r = 0.24$, $p > 0.1$) (Fig. 6c).

The relationship between $\delta^{18}\text{O}$ and temperature is much stronger over the adjacent ocean (Fig. 5d). The spatial correlation plot reveals a positive correlation with 2 m temperature over the Bellingshausen Sea ($r > 0.6$) within the approximate area of the seasonal sea ice zone.

3.6 Major ions

As expected for an island location, the major ions deposited at Peter I are largely of marine origin. The ratio of $\text{Cl}^- / \text{Na}^+$ in the ice core is 1.8, consistent with the standard seawater ratio (1.79). Thus, at this site $[\text{Na}^+]$ can be considered primarily of marine origin ($\sim 95\%$). The $\text{Cl}^- / \text{Mg}^{2+}$ and $\text{Cl}^- / \text{Ca}^{2+}$ ratios suggest that seawater accounts for 82% and 73% of the $[\text{Mg}^{2+}]$ and $[\text{Ca}^{2+}]$, respectively.

The average $[\text{Na}^+]$ at Peter I Island is 998 ppb, consistent with a coastal location. A database of 105 Antarctic ice cores (Thomas et al., 2023) suggests that the highest $[\text{Na}^+]$ in an Antarctic ice core is observed on the Fimbul Ice Shelf in coastal East Antarctica, where average concentrations exceed 2700 ppb. The average $[\text{Na}^+]$ at Peter I Island is higher than the sub-Antarctic Bouvet Island in the South Atlantic, where the average $[\text{Na}^+]$ was 101 ppb (King et al., 2019). It is also higher than values on the Antarctic Peninsula, which range between 50–215 ppb (Emanuelsson et al., 2022; Thomas et al., 2022); however, the drill sites are higher in elevation and further from the oceanic source.

The average $[\text{SO}_4^{2-}]$ at Peter I Island is 267 ppb. This is considerably higher than concentrations found in Antarctic Peninsula ice cores, where values of between ~ 30 and 70 ppb are observed (Thomas et al., 2023; Emanuelsson et al., 2022). However, higher concentrations are observed at

Bouvet Island (King et al., 2019) (529 ppb) and the Fimbul Ice Shelf (536 ppb) (Thomas et al., 2023).

4 Discussion

The objective of this study is to establish if a firn core from Peter I Island is suitable for paleoclimate reconstructions. Here we discuss the climatological data captured by the firn core and explore this site's potential for future deep-ice-core drilling.

4.1 Annual-layer counted age-scale

We have established that seasonal cycles in D_{xs} , major ion chemistry, and $\delta^{18}\text{O}$ are suitable for annual-layer counting. This has been verified using a prominent peak in $[\text{SO}_4^{2-}]$ and evidence for cryptotephra shards corresponding to the Puyehue–Cordón Caulle eruption in 2011 (Koffman et al., 2017). The lack of evidence (in both $[\text{SO}_4^{2-}]$ and cryptotephra) of the Sturge Island eruption in 2001, visible at proximal sites on the Antarctic Peninsula (Tetzner et al., 2001), suggests that this record does not extend beyond 2002. The volcanic reference horizons provide independent age constraints in approximately the middle (2012) and lower (2002) sections of the firn core.

In addition to the volcanic reference horizons, the location of prominent melt features further supports the age scale. The two largest melt features occur in the layers assigned to 2012 and 2006, which can be explained by the two warmest years in the ERA5 temperature record (2002–2016) occurring in 2013 and 2006. The downward percolation of meltwater generated in January 2013 means that the melt feature is observed in the annual layer assigned as 2012 (Fig. 4). The AWS data reveal that positive degree days, expected to result in surface melting, did occur for a prolonged period during February and March 2006. The high correlation ($r = 0.73$, $p > 0.01$) between the annual melt layer thickness and maximum daily 2 m temperatures from ERA5 provides further evidence to support the age scale.

An estimated bottom age of 2004 ± 2 years was proposed in Thomas et al. (2021) based on the Herron and Langway densification model (Herron and Langway, 1980) and applied to the measured density profile and $P-E$ from ERA5. When using the newly calculated snow accumulation ($0.49 \text{ m w.e. yr}^{-1}$), the updated density-derived bottom age is 2002 ± 1 years. This is within the uncertainty of the previous estimate derived using an upper (annual $P-E$ plus 1 standard deviation) and lower (annual $P-E$ minus 1 standard deviation) $P-E$ value (Thomas et al., 2021), thus validating the use of the densification model to estimate the potential bottom age for a deeper ice core. The density profile estimate suggests that an ice core drilled to the maximum GPR layer depth (identified at 43 m; Thomas et al., 2021) would provide a record dating back to 1951 CE ± 5 years. While the ice cap thickness remains unknown based on the measured snow ac-

cumulation rate and density profile, we conclude that an ice core drilled to 100 m depth would provide a record dating back to 1833 CE ± 13 years.

4.2 Proxy validation and comparison with reanalysis (ERA5)

As we only have a single AWS temperature record that does not comprise a full year and is some distance from the ice core site, we must rely on the reanalysis data to evaluate our proxy measurements. The previous ECMWF reanalysis products (ERA-Interim and ERA-40) have been tested widely in Antarctica (e.g. Bromwich and Fogt, 2004) and at sites in the adjacent Ellsworth Land coast and the Antarctic Peninsula (Thomas and Bracegirdle, 2009, 2015). A recent study confirms that ERA5 accurately captures variability across Antarctica (Zhu et al., 2021) and in near-surface air temperature and wind regimes over the adjacent Antarctic Peninsula (Tetzner et al., 2019). The AWS data from Peter I Island provide an opportunity to expand this previous research to incorporate a sub-Antarctic Island.

The high correlation between daily mean 2 m temperature in ERA5 and temperature recorded at an AWS demonstrate the high degree of skill in ERA5 at this location. The correlation of 0.91 is consistent with the correlation of 0.92 determined when comparing observations and ERA5 annual mean temperatures for Antarctica (Zhu et al., 2021). However, in the absence of a measured lapse rate it is difficult to determine the true temperature bias in the ERA5 reanalysis for Peter I Island. If we apply the lapse rate of $0.32\text{--}0.44 \text{ }^\circ\text{C } 100 \text{ m}^{-1}$ (proposed in Sect. 3.2) this suggests that ERA5 has a warm bias of $\sim 0.52\text{--}0.67 \text{ }^\circ\text{C}$.

Comparing the 15 years of annual mean snow accumulation from the firn core with $P-E$ from ERA5 (Fig. 4a) revealed a high temporal correlation between the two records ($r = 0.75$, $p < 0.01$) and comparable absolute values. The slight overestimation of the ERA5 total $P-E$ ($\sim 4\text{--}6\%$) is less than the offset observed at adjacent sites on the Antarctic Peninsula (Thomas and Bracegirdle, 2009, 2015). Differences between snow accumulation and $P-E$ are expected due to the post-deposition processes including melt and windblown deposition and erosion. In addition, the resolution of the ERA5 reanalysis data (0.25° resolution, $\sim 31 \text{ km}$) is not sufficient to differentiate Peter I Island from the surrounding ocean. However, despite this limitation our study suggests that ERA5 displays a high degree of skill in capturing the absolute amount of precipitation and the temporal variability in precipitation changes at this firn core site on a small and mountainous island location. Importantly, the spatial correlation maps reveal that the high correlation between snow accumulation and ERA5 $P-E$ extends over the Antarctic Peninsula and Amundsen Sea–Bellingshausen Sea region (Fig. 4b). These results support the use of the firn core for regional climate reconstructions.

4.3 Relationship between snow accumulation and stable isotopes with precipitation and temperature

The strong correlation ($r = 0.75$, $p < 0.01$) between annual snow accumulation and $P-E$ in the corresponding ERA5 grid cell over the common 15-year interval suggests that the ice core layer thickness (snow accumulation) is dominated by changes in precipitation. Thus, a longer reconstruction could provide valuable insight into changes in snow accumulation and surface mass balance across a large and dynamic region of Antarctica. Although traditionally viewed as a proxy for past surface temperature, the annual-average $\delta^{18}\text{O}$ at this site is not correlated with site annual-average ERA5 2 m temperature (0.24 , $p = 0.17$). However, the observed weak correlation coefficients ($\delta^{18}\text{O}$ vs. 2 m surface air temperature) are consistent with ice cores from the Antarctic Peninsula and coastal Ellsworth Land (e.g. Thomas et al., 2009, 2013).

At Peter I Island, the annual snow accumulation is related to annual ERA5 2 m surface air temperatures. The positive correlation between snow accumulation and ERA5 2 m T ($r = 0.59$, $p < 0.03$) reflects the relationship between temperature and the saturation water vapour pressure governed by the Clausius–Clapeyron relation. This relationship has been observed at ice core sites across the Antarctic Peninsula (e.g. Thomas et al., 2017) and confirmed at the continental scale (Medley and Thomas., 2019) and in a data assimilation approach using global circulation models (Dalaiden et al., 2021). In the correlation map (Fig. 4d), there is a significant region of correlation between $\delta^{18}\text{O}$ and 2 m temperatures over the adjacent ocean, especially within the seasonal sea ice zone. This suggests that sea ice may play a role in modulating $\delta^{18}\text{O}$ at this site. Sea ice has been shown to directly alter $\delta^{18}\text{O}$ through an enrichment of the water vapour (Bromwich and Weaver, 1983). A reduction in the length of the sea ice season and an overall decline in sea ice coverage in the Amundsen and Bellingshausen seas has been attributed to the warming trends observed in previous West Antarctic reconstructions (Küttel et al., 2012; Steig et al., 2009; Thomas et al., 2013). Thus, we conclude that over longer timescales $\delta^{18}\text{O}$ and snow accumulation from any future ice cores from this site will capture changes in surface air temperatures in this region.

4.4 Drivers of variability and the influence of atmospheric modes

The record is too short to draw robust conclusions about the role of large-scale atmospheric circulation. However, given the island's location we expect this site to be strongly influenced by the Amundsen Sea Low (ASL), a climatological low-pressure system that exerts considerable influence on the climate of West Antarctica (Hosking et al., 2013). Pressure in the ASL region is strongly modulated by large-scale modes of variability, especially the Southern Annular Mode (SAM) and El Niño–Southern Oscillation (ENSO) (Fogt et

al., 2012; Hosking et al., 2013). Enhanced northerly flow over the Bellingshausen Sea during the positive phase of the SAM has been attributed to the large increase in snowfall on the Antarctic Peninsula during the late 20th century (e.g. Thomas et al., 2008, 2015, 2017; Medley and Thomas, 2019). Back-trajectory analysis suggests that air masses reaching the Antarctic Peninsula passed over Peter I Island (Thomas and Bracegirdle, 2015), suggesting similar climate drivers are likely to influence snowfall at Peter I Island. Given the evidence from back-trajectory analysis that air masses reaching the Antarctic Peninsula pass over Peter I Island (Thomas and Bracegirdle, 2015), it is likely that the two locations will be influenced by similar climate drivers. However, the short duration of the records limits further evaluation of the role of SAM and ENSO, which has been proven to vary temporally at many sites across West Antarctica (Thomas et al., 2015; Wang et al., 2017).

4.5 Drivers of surface melt and the impact on proxy preservation

Despite its maritime location, Peter I Island is situated south of the polar front at a comparable latitude to much of the East Antarctic coastline ($\sim 70^\circ\text{S}$). While the annual-average temperature (1979–2017) is -9.5°C , with summer temperatures of -5.1°C (Thomas et al., 2021), the daily temperatures from ERA5 indicate maximum temperature at the site has exceeded 3°C . This maximum in February 2006 was verified by in situ observations from an AWS. Over the 15-year period (~ 5500 d) covered by the firn core, there were a total of 189 positive degree days. Many (but not all) of these positive degree days correspond to visible melt layers in the ice core. However, there are some notable exceptions where melt features do not coincide with positive degree days.

Many of the major melt periods also coincide with documented evidence of atmospheric rivers (ARs). These narrow bands of enhanced water vapour transport heat and moisture from mid-latitudes to high latitudes and have been attributed to melt events across West Antarctica (Nicolas et al., 2017). Wille et al. (2019) derived an AR detection algorithm to demonstrate that between 40%–80% of surface melt on the western Antarctic Peninsula (1979–2017) can be attributed to ARs that make landfall during the winter months (March–October). Many of the ARs identified in that study pass directly over Peter I Island, with the two most abundant AR years, 2006 and 2013, coincident with the strongest melt features in the firn core. The year 2010 also contained a high number of AR occurrences; however, this year does not correspond to any major melt features in our record. However, 2010 was a high snow accumulation year, and the enhanced moisture transport characterized by ARs is also known to increase precipitation. The physical mechanisms relating ARs to surface melt are complex, and thus it may be possible that some ARs passing over Peter I result in increased precipitation but not visible melt features or that the ARs during 2010

that made landfall in West Antarctica did not pass directly over Peter I Island.

There is some evidence that the chemical and isotopic records during the extreme melt event in 2012 have been altered. This is observed in the near-homogeneous concentrations of major ion and $\delta^{18}\text{O}$ values during this melt feature (Fig. 2), which appear to have removed the seasonal signal. Meltwater percolation in the firn is known to elute soluble ions and make $\delta^{18}\text{O}$ appear smoothed (Moser et al., 2024). The occurrence of melt has also likely increased the uncertainty in the snow accumulation calculations. However, it is only during the most extreme years that melt has had a notable impact on the proxy preservation. A high-resolution evaluation of the melt features and their impact on chemical elution is a subject for further study.

Instrumental records from the Antarctic Peninsula suggest that annual surface air temperatures have increased by approximately $2.5\text{ }^{\circ}\text{C}$ since the 1950s (Turner et al., 2005), with reports of record-breaking heatwaves in recent years (González-Herrero et al., 2022). This warming is corroborated by ice core records across the Antarctic Peninsula and coastal Ellsworth Land, which suggest a prominent warming trend during the latter half of the 20th century (Thomas et al., 2013, 2009; Thomas and Tetzner, 2018). Despite the absence of a significant warming trend during the 21st century (Turner et al., 2016), the temperatures during the 21st century are still considerably warmer than the early and middle 20th century. Thus, we might expect that the melt frequency observed during this period (2002–2016) will also be much higher than at any time in the recent past. A deeper ice core drilled from this location may be subject to melting in the surface layers due to continued regional warming (González-Herrero et al., 2022), although the impact of melting is likely limited to the middle 20th century onwards.

This hypothesis is supported by the melt history obtained from the James Ross Island (JRI) ice core at the northeastern tip of the Antarctic Peninsula (Abram et al., 2013). Mean annual temperatures of $-14.3\text{ }^{\circ}\text{C}$ were reported at the JRI site during the 1980s (Aristarain et al., 1987); however, during the period 2001–2017 the annual-average temperature increased to $-7.5\text{ }^{\circ}\text{C}$, which is warmer than the $-9.5\text{ }^{\circ}\text{C}$ observed at Peter I Island. This may explain why the average melt layer thickness of 3.2 cm yr^{-1} at JRI is higher than the observed 1.8 cm per year at Peter I Island. The visible melt features at JRI display a clear acceleration in frequency during the late 20th century (Abram et al., 2013). However, this melt has not had a notable influence on the proxy preservation or subsequent paleoclimate reconstructions generated from this site (e.g. Abram et al., 2013).

5 Conclusions

Here we present the first climatic interpretation of $\delta^{18}\text{O}$ and snow accumulation data contained in a firn core drilled on the

remote sub-Antarctic Peter I Island. We conclude that a deep ice core from this site has the potential to provide valuable paleoclimate reconstructions, exploring the ice–atmosphere–ocean interactions in the Bellingshausen Sea, based on the following findings.

- The firn core can be counted in terms of annual layers and verified using a volcanic reference horizon from the Puyehue–Cordón Caulle eruption in 2011.
- The ERA5 reanalysis displays a high degree of skill at reproducing site surface temperature and snow accumulation. This is confirmed by comparing daily temperatures from an AWS against ERA5 2 m temperatures and by comparing annual-average snow accumulation from the ice core against annual-average precipitation ($P-E$) from ERA5 at the corresponding grid cell. This demonstrates that ERA5 can capture climate variability even at a small sub-Antarctic island and supports the use of ERA5 as a suitable dataset to interpret climate proxies in this firn core.
- Snow accumulation observed in the firn core is significantly correlated to both regional precipitation ($P-E$) changes and changes in surface air temperature.
- Snow accumulation at the firn core site is likely related to large-scale modes of atmospheric variability, including SAM. However, the stability of the relationship between SAM and snow accumulation cannot be confirmed beyond the 15-year interval of the firn core.
- The $\delta^{18}\text{O}$ record, although weakly correlated with site temperature, displays a relationship with air temperature over the seasonal sea ice zone in the Bellingshausen Sea.
- The melt frequency is lower than observed at existing deep-ice-core sites from coastal Antarctica. The melt features correlate with maximum daily temperature, with the two most extreme melt years (2006 and 2012) coincident with high temperatures and the documented occurrence of atmospheric rivers (in 2006 and 2013).
- While the ice cap thickness remains unknown, based on the measured snow accumulation rate and density profile we conclude that an ice core drilled to 100 m depth would capture climate variability of the past ~ 200 years.

Data availability. All data have been submitted to the UK Polar Data Centre and are available upon request (lith@bas.ac.uk) or from the following address: <https://doi.org/10.5285/6c28fe74-1a14-42ac-ae60-c2bc05c360b6> (Thomas, 2024).

Author contributions. ERT designed the project and prepared the manuscript with contributions from all authors. JP, BM, and GG conducted the fieldwork; DT produced the age scale; DEM contributed to the sample preparation; and SJ conducted the IC analysis.

Competing interests. At least one of the (co-)authors is a member of the editorial board of *Climate of the Past*. The peer-review process was guided by an independent editor, and the authors also have no other competing interests to declare.

Disclaimer. Publisher's note: Copernicus Publications remains neutral with regard to jurisdictional claims made in the text, published maps, institutional affiliations, or any other geographical representation in this paper. While Copernicus Publications makes every effort to include appropriate place names, the final responsibility lies with the authors.

Special issue statement. This article is part of the special issue "Ice core science at the three poles (CP/TC inter-journal SI)". It is a result of the IPICS 3rd Open Science Conference, Crans-Montana, Switzerland, 2–7 October 2022.

Acknowledgements. Funding was provided to subICE by École Polytechnique Fédérale de Lausanne, the Swiss Polar Institute, and Ferring Pharmaceuticals Inc. Elizabeth R. Thomas received core funding from the Natural Environment Research Council to the British Antarctic Survey's Ice Dynamics and Palaeoclimate programme. Joel B. Pedro acknowledges support from the European Research Council under the European Community's Seventh Framework Programme (FP7/2007e2013) and ERC grant agreement no. 610055 as part of the ice2ice project and from the Australian Government Department of Industry Science Energy and Resources (grant no. ASCI000002). We are grateful to the Norwegian Polar Institute for granting us permission to visit Peter I Island. The authors appreciate the support of the University of Wisconsin–Madison Automatic Weather Station Program for the dataset, data display, and information (NSF grant no. 1924730) and ECMWF for providing ERA5 reanalysis data. We thank Laura Gerish (BAS) for producing the maps. We thank Joe Brown and Daniel Emanuelsson for the line-scanning image. Data used in this study are available through the UK Polar Data Centre. The authors would like to acknowledge the coordinators and participants of the Antarctic Circumnavigation Expedition for facilitating collection of the subICE cores, especially David Walton, Christian de Marliave, Julia Schmale, Robert Brett, Sergio Rodrigues, Francois Bernard, Amy King, Roger Stilwell, and Frederick Paulsen. We thank the three anonymous reviewers and the editor for their constructive feedback.

Financial support. This research has been supported by the École Polytechnique Fédérale de Lausanne (ACE project 4 and Swiss Polar Institute) and the Natural Environment Research Council (Core funding).

Review statement. This paper was edited by Paolo Gabrielli and reviewed by Bess Koffman and three anonymous referees.

References

- Abram, N. J., Thomas, E. R., McConnell, J. R., Mulvaney, R., Bracegirdle, T. J., Sime, L. C., and Aristarain, A. J.: Ice core evidence for a 20th century decline in sea ice in the Bellingshausen Sea, Antarctica, *J. Geophys. Res.*, 115, D23101, <https://doi.org/10.1029/2010JD014644>, 2010.
- Abram, N. J., Mulvaney, R., Wolff, E. W., Triest, J., Kipfstuhl, S., Trusel, L. D., Vimeux, F., Fleet, L., and Arrowsmith, C.: Acceleration of snow melt in an Antarctic Peninsula ice core during the twentieth century, *Nat. Geosci.*, 6, 404–411, <https://doi.org/10.1038/ngeo1787>, 2013.
- Aristarain, A. J., Pinglot, J. F., and Pourchet, M.: Accumulation and Temperature Measurements on the James Ross Island Ice Cap, Antarctic Peninsula, Antarctica, *J. Glaciol.*, 33, 357–362, <https://doi.org/10.3189/S0022143000008959>, 1987.
- Bromwich, D. H. and Fogt, R. L.: Strong Trends in the Skill of the ERA-40 and NCEP–NCAR Reanalyses in the High and Midlatitudes of the Southern Hemisphere, 1958–2001, *J. Climate*, 17, 4603–4619, <https://doi.org/10.1175/3241.1>, 2004.
- Bromwich, D. H. and Weaver, C. J.: Latitudinal displacement from main moisture source controls $\delta^{18}\text{O}$ of snow in coastal Antarctica, *Nature*, 301, 145–147, <https://doi.org/10.1038/301145a0>, 1983.
- Dalaiden, Q., Goosse, H., Rezsöhazy, J., and Thomas, E. R.: Reconstructing atmospheric circulation and sea-ice extent in the West Antarctic over the past 200 years using data assimilation, *Clim. Dynam.*, 57, 3479–3503, <https://doi.org/10.1007/s00382-021-05879-6>, 2021.
- Emanuelsson, B. D., Thomas, E. R., Tetzner, D. R., Humby, J. D., and Vladimirova, D. O.: Ice Core Chronologies from the Antarctic Peninsula: The Palmer, Jurassic, and Rendezvous Age-Scales, *Geosciences*, 12, 87, <https://doi.org/10.3390/geosciences12020087>, 2022.
- Fernandoy, F., Meyer, H., and Tonelli, M.: Stable water isotopes of precipitation and firn cores from the northern Antarctic Peninsula region as a proxy for climate reconstruction, *The Cryosphere*, 6, 313–330, <https://doi.org/10.5194/tc-6-313-2012>, 2012.
- Fernandoy, F., Tetzner, D., Meyer, H., Gacitúa, G., Hoffmann, K., Falk, U., Lambert, F., and MacDonell, S.: New insights into the use of stable water isotopes at the northern Antarctic Peninsula as a tool for regional climate studies, *The Cryosphere*, 12, 1069–1090, <https://doi.org/10.5194/tc-12-1069-2018>, 2018.
- Fitzgerald, N. B. and Kirkpatrick, J. B.: Air temperature lapse rates and cloud cover in a hyper-oceanic climate, *Antarct. Sci.*, 32, 440–453, <https://doi.org/10.1017/S0954102020000309>, 2020.
- Fogt, R. L., Jones, J. M., and Renwick, J.: Seasonal zonal asymmetries in the Southern Annular Mode and their impact on regional temperature anomalies, *J. Climate*, 25, 6253–6270, 2012.
- González-Herrero, S., Barriopedro, D., Trigo, R. M., López-Bustins, J. A., and Oliva, M.: Climate warming amplified the 2020 record-breaking heatwave in the Antarctic Peninsula, *Commun. Earth Environ.*, 3, 122, <https://doi.org/10.1038/s43247-022-00450-5>, 2022.
- Goodwin, B. P., Mosley-Thompson, E., Wilson, A. B., Porter, S. E., and Sierra-Hernandez, M. R.: Accumulation Variability in

- the Antarctic Peninsula: The Role of Large-Scale Atmospheric Oscillations and Their Interactions, *J. Climate*, 29, 2579–2596, <https://doi.org/10.1175/jcli-d-15-0354.1>, 2016.
- Hatvani, I. G., Leuenberger, M., Kohán, B., and Kern, Z.: Geostatistical analysis and isoscape of ice core derived water stable isotope records in an Antarctic macro region, *Polar Sci.*, 13, 23–32, 2017.
- Herron, M. M. and Langway, C. C.: Firn Densification – an Empirical-Model, *J. Glaciol.*, 25, 373–385, <https://doi.org/10.3189/S0022143000015239>, 1980.
- Hersbach, H., Bell, B., Berrisford, P., Hirahara, S., Horányi, A., Muñoz-Sabater, J., Nicolas, J., Peubey, C., Radu, R., Schepers, D., Simmons, A., Soci, C., Abdalla, S., Abellan, X., Balsamo, G., Bechtold, P., Biavati, G., Bidlot, J., Bonavita, M., De Chiara, G., Dahlgren, P., Dee, D., Diamantakis, M., Dragani, R., Fleming, J., Forbes, R., Fuentes, M., Geer, A., Haimberger, L., Healy, S., Hogan, R. J., Hólm, E., Janisková, M., Keeley, S., Laloyaux, P., Lopez, P., Lupu, C., Radnoti, G., de Rosnay, P., Rozum, I., Vamborg, F., Villaume, S., and Thépaut, J.-N.: The ERA5 global reanalysis, *Q. J. Roy. Meteor. Soc.*, 146, 1999–2049, <https://doi.org/10.1002/qj.3803>, 2020.
- Hosking, J. S., Orr, A., Marshall, G. J., Turner, J., and Phillips, T.: The Influence of the Amundsen–Bellingshausen Seas Low on the Climate of West Antarctica and Its Representation in Coupled Climate Model Simulations, *J. Climate*, 26, 6633–6648, <https://doi.org/10.1175/jcli-d-12-00813.1>, 2013.
- Jenkins, A. and Jacobs, S.: Circulation and melting beneath George VI Ice Shelf, Antarctica, *J. Geophys. Res.-Oceans*, 113, C04013, <https://doi.org/10.1029/2007JC004449>, 2008.
- King, A. C. F., Thomas, E. R., Pedro, J. B., Markle, B., Potocki, M., Jackson, S. L., Wolff, E., and Kalberer, M.: Organic Compounds in a Sub-Antarctic Ice Core: A Potential Suite of Sea Ice Markers, *Geophys. Res. Lett.*, 46, 9930–9939, <https://doi.org/10.1029/2019GL084249>, 2019.
- Koffman, B. G., Dowd, E. G., Osterberg, E. C., Ferris, D. G., Hartman, L. H., Wheatley, S. D., Kurbatov, A. V., Wong, G. J., Markle, B. R., Dunbar, N. W., Kreutz, K. J., and Yates, M.: Rapid transport of ash and sulfate from the 2011 Puyehue-Cordon Caulle (Chile) eruption to West Antarctica, *J. Geophys. Res.-Atmos.*, 122, 8908–8920, <https://doi.org/10.1002/2017jd026893>, 2017.
- Küttel, M., Steig, E. J., Ding, Q., Monaghan, A. J., and Battisti, D. S.: Seasonal climate information preserved in West Antarctic ice core water isotopes: relationships to temperature, large-scale circulation, and sea ice, *Clim. Dynam.*, 39, 1841–1857, <https://doi.org/10.1007/s00382-012-1460-7>, 2012.
- Lenaerts, J. T. M. and van den Broeke, M. R.: Modeling drifting snow in Antarctica with a regional climate model: 2. Results, *J. Geophys. Res.-Atmos.*, 117, D05109, <https://doi.org/10.1029/2010JD015419>, 2012.
- Li, C., Michel, C., Seland Graff, L., Bethke, I., Zappa, G., Bracegirdle, T. J., Fischer, E., Harvey, B. J., Iversen, T., King, M. P., Krishnan, H., Lierhammer, L., Mitchell, D., Scinocca, J., Shiogama, H., Stone, D. A., and Wettstein, J. J.: Midlatitude atmospheric circulation responses under 1.5 and 2.0 °C warming and implications for regional impacts, *Earth Syst. Dynam.*, 9, 359–382, <https://doi.org/10.5194/esd-9-359-2018>, 2018.
- Markle, B. R. and Steig, E. J.: Improving temperature reconstructions from ice-core water-isotope records, *Clim. Past*, 18, 1321–1368, <https://doi.org/10.5194/cp-18-1321-2022>, 2022.
- Martin, P. J. and Peel, D. A.: The Spatial Distribution of 10 m Temperatures in the Antarctic Peninsula, *J. Glaciol.*, 20, 311–317, <https://doi.org/10.3189/S0022143000013861>, 1978.
- Medley, B. and Thomas, E. R.: Increased snowfall over the Antarctic Ice Sheet mitigated twentieth-century sea-level rise, *Nat. Clim. Change*, 9, 34–39, <https://doi.org/10.1038/s41558-018-0356-x>, 2019.
- Moser, D. E., Jackson, S., Kjær, H. A., Markle, B., Ngoumtsa, E., Pedro, J. B., Segato, D., Spolaor, A., Tetzner, D., Vallelonga, P., and Thomas, E. R.: An Age Scale for the First Shallow (Sub-)Antarctic Ice Core from Young Island, Northwest Ross Sea, *Geosciences*, 11, 368, <https://doi.org/10.3390/geosciences11090368>, 2021.
- Moser, D. E., Thomas, E. R., Nehrbass-Ahles, C., Eichler, A., and Wolff, E.: Review article: Melt-affected ice cores for polar research in a warming world, *The Cryosphere*, 18, 2691–2718, <https://doi.org/10.5194/tc-18-2691-2024>, 2024.
- Münch, T., Kipfstuhl, S., Freitag, J., Meyer, H., and Laeple, T.: Constraints on post-depositional isotope modifications in East Antarctic firn from analysing temporal changes of isotope profiles, *The Cryosphere*, 11, 2175–2188, <https://doi.org/10.5194/tc-11-2175-2017>, 2017.
- Nicolas, J. P., Vogelmann, A. M., Scott, R. C., Wilson, A. B., Cadeddu, M. P., Bromwich, D. H., Verlinde, J., Lubin, D., Russell, L. M., Jenkinson, C., Powers, H. H., Ryczek, M., Stone, G., and Wille, J. D.: January 2016 extensive summer melt in West Antarctica favoured by strong El Niño, *Nat. Commun.*, 8, 15799, <https://doi.org/10.1038/ncomms15799>, 2017.
- Nyakatya, M. and McGeoch, M. A.: Temperature variation across Marion Island associated with a keystone plant species (*Azorella selago* Hook. (Apiaceae)), *Polar Biol.*, 31, 139–151, 2008.
- Nye, J. F.: Correction factor for accumulation measured by the thickness of the annual layers in an ice sheet, *J. Glaciol.*, 4, 785–788, 1963.
- Ó Cofaigh, C., Larter, R. D., Dowdeswell, J. A., Hillenbrand, C.-D., Pudsey, C. J., Evans, J., and Morris, P.: Flow of the West Antarctic Ice Sheet on the continental margin of the Bellingshausen Sea at the Last Glacial Maximum, *J. Geophys. Res.-Sol. Ea.*, 110, B11103, <https://doi.org/10.1029/2005JB003619>, 2005.
- Paolo, F. S., Fricker, H. A., and Padman, L.: Volume loss from Antarctic ice shelves is accelerating, *Science*, 348, 327–331, <https://doi.org/10.1126/science.aaa0940>, 2015.
- Parkinson, C. L.: A 40-y record reveals gradual Antarctic sea ice increases followed by decreases at rates far exceeding the rates seen in the Arctic, *P. Natl. Acad. Sci. USA*, 116, 14414–14423, <https://doi.org/10.1073/pnas.1906556116>, 2019.
- Porter, S. E., Parkinson, C. L., and Mosley-Thompson, E.: Bellingshausen Sea ice extent recorded in an Antarctic Peninsula ice core, *J. Geophys. Res.-Atmos.*, 121, 13886–813900, <https://doi.org/10.1002/2016JD025626>, 2016.
- Pritchard, H. D., Arthern, R. J., Vaughan, D. G., and Edwards, L. A.: Extensive dynamic thinning on the margins of the Greenland and Antarctic ice sheets, *Nature*, 461, 971–975, <https://doi.org/10.1038/nature08471>, 2009.

- Purich, A. and Doddridge, E. W.: Record low Antarctic sea ice coverage indicates a new sea ice state, *Commun. Earth Environ.*, 4, 314, <https://doi.org/10.1038/s43247-023-00961-9>, 2023.
- Royles, J., Amesbury, Matthew J., Convey, P., Griffiths, H., Hodgson, Dominic A., Leng, Melanie J., and Charman, Dan J.: Plants and Soil Microbes Respond to Recent Warming on the Antarctic Peninsula, *Curr. Biol.*, 23, 1702–1706, <https://doi.org/10.1016/j.cub.2013.07.011>, 2013.
- Siegert, M., Atkinson, A., Banwell, A., Brandon, M., Convey, P., Davies, B., Downie, R., Edwards, T., Hubbard, B., Marshall, G., Rogelj, J., Rumble, J., Stroeve, J., and Vaughan, D.: The Antarctic Peninsula Under a 1.5 °C Global Warming Scenario, *Frontiers in Environmental Science*, 7, 102, <https://doi.org/10.3389/fenvs.2019.00102>, 2019.
- Smith, B., Fricker, H. A., Gardner, A. S., Medley, B., Nilsson, J., Paolo, F. S., Holschuh, N., Adusumilli, S., Brunt, K., Csatho, B., Harbeck, K., Markus, T., Neumann, T., Siegfried, M. R., and Zwally, H. J.: Pervasive ice sheet mass loss reflects competing ocean and atmosphere processes, *Science*, 368, 1239–1242, <https://doi.org/10.1126/science.aaz5845>, 2020.
- Steig, E. J., Schneider, D. P., Rutherford, S. D., Mann, M. E., Comiso, J. C., and Shindell, D. T.: Warming of the Antarctic ice-sheet surface since the 1957 International Geophysical Year, *Nature*, 457, 459–462, <https://doi.org/10.1038/nature07669>, 2009.
- Stenni, B., Curran, M. A. J., Abram, N. J., Orsi, A., Goursaud, S., Masson-Delmotte, V., Neukom, R., Goosse, H., Divine, D., van Ommen, T., Steig, E. J., Dixon, D. A., Thomas, E. R., Bertler, N. A. N., Isaksson, E., Ekaykin, A., Werner, M., and Frezzotti, M.: Antarctic climate variability on regional and continental scales over the last 2000 years, *Clim. Past*, 13, 1609–1634, <https://doi.org/10.5194/cp-13-1609-2017>, 2017.
- Tetzner, D., Thomas, E., and Allen, C.: A Validation of ERA5 Reanalysis Data in the Southern Antarctic Peninsula–Ellsworth Land Region, and Its Implications for Ice Core Studies, *Geosciences*, 9, 289, <https://doi.org/10.3390/geosciences9070289>, 2019.
- Tetzner, D. R., Thomas, E. R., Allen, C. S., and Piermattei, A.: Evidence of Recent Active Volcanism in the Balleny Islands (Antarctica) From Ice Core Records, *J. Geophys. Res.-Atmos.*, 126, e2021JD035095, <https://doi.org/10.1029/2021JD035095>, 2021.
- Tetzner, D. R., Allen, C. S., and Thomas, E. R.: Regional variability of diatoms in ice cores from the Antarctic Peninsula and Ellsworth Land, *Antarctica, The Cryosphere*, 16, 779–798, <https://doi.org/10.5194/tc-16-779-2022>, 2022.
- Thomas, E.: Major ion chemistry, stable water isotopes and snow accumulation from the Peter 1st firn core, 2002–2017 (Version 1.0), NERC EDS UK Polar Data Centre [data set], <https://doi.org/10.5285/6c28fe74-1a14-42ac-ae60-c2bc05c360b6>, 2024.
- Thomas, E. R. and Abram, N. J.: Ice core reconstruction of sea ice change in the Amundsen-Ross Seas since 1702 A.D., *Geophys. Res. Lett.*, 43, 5309–5317, <https://doi.org/10.1002/2016GL068130>, 2016.
- Thomas, E. R. and Bracegirdle, T. J.: Improving ice core interpretation using in situ and reanalysis data, *J. Geophys. Res.-Atmos.*, 114, D20116, <https://doi.org/10.1029/2009jd012263>, 2009.
- Thomas, E. R. and Bracegirdle, T. J.: Precipitation pathways for five new ice core sites in Ellsworth Land, West Antarctica, *Clim. Dyn.*, 44, 2067–2078, <https://doi.org/10.1007/s00382-014-2213-6>, 2015.
- Thomas, E. R. and Tetzner, D. R.: The Climate of the Antarctic Peninsula during the Twentieth Century: Evidence from Ice Cores, *IntechOpen*, <https://doi.org/10.5772/intechopen.81507>, 2018.
- Thomas, E. R., Marshall, G. J., and McConnell, J. R.: A doubling in snow accumulation in the western Antarctic Peninsula since 1850, *Geophys. Res. Lett.*, 35, L01706, <https://doi.org/10.1029/2007GL032529>, 2008.
- Thomas, E. R., Dennis, P. F., Bracegirdle, T. J., and Franzke, C.: Ice core evidence for significant 100-year regional warming on the Antarctic Peninsula, *Geophys. Res. Lett.*, 36, L20704, <https://doi.org/10.1029/2009GL040104>, 2009.
- Thomas, E. R., Bracegirdle, T. J., Turner, J., and Wolff, E. W.: A 308 year record of climate variability in West Antarctica, *Geophys. Res. Lett.*, 40, 5492–5496, <https://doi.org/10.1002/2013gl057782>, 2013.
- Thomas, E. R., Hosking, J. S., Tuckwell, R. R., Warren, R. A., and Ludlow, E. C.: Twentieth century increase in snowfall in coastal West Antarctica, *Geophys. Res. Lett.*, 42, 9387–9393, <https://doi.org/10.1002/2015gl065750>, 2015.
- Thomas, E. R., van Wessem, J. M., Roberts, J., Isaksson, E., Schlosser, E., Fudge, T. J., Vallelonga, P., Medley, B., Lenaerts, J., Bertler, N., van den Broeke, M. R., Dixon, D. A., Frezzotti, M., Stenni, B., Curran, M., and Ekaykin, A. A.: Regional Antarctic snow accumulation over the past 1000 years, *Clim. Past*, 13, 1491–1513, <https://doi.org/10.5194/cp-13-1491-2017>, 2017.
- Thomas, E. R., Allen, C. S., Etourneau, J., King, A. C. F., Severi, M., Winton, V. H. L., Mueller, J., Crosta, X., and Peck, V. L.: Antarctic Sea Ice Proxies from Marine and Ice Core Archives Suitable for Reconstructing Sea Ice over the Past 2000 Years, *Geosciences*, 9, 506, <https://doi.org/10.3390/geosciences9120506>, 2019.
- Thomas, E. R., Gacitúa, G., Pedro, J. B., Faith King, A. C., Markle, B., Potocki, M., and Moser, D. E.: Physical properties of shallow ice cores from Antarctic and sub-Antarctic islands, *The Cryosphere*, 15, 1173–1186, <https://doi.org/10.5194/tc-15-1173-2021>, 2021.
- Thomas, E. R., Vladimirova, D. O., Tetzner, D. R., Emanuelsson, B. D., Chellman, N., Dixon, D. A., Goosse, H., Grieman, M. M., King, A. C. F., Sigl, M., Udy, D. G., Vance, T. R., Winski, D. A., Winton, V. H. L., Bertler, N. A. N., Hori, A., Laluraj, C. M., McConnell, J. R., Motizuki, Y., Takahashi, K., Motoyama, H., Nakai, Y., Schwanck, F., Simões, J. C., Lindau, F. G. L., Severi, M., Traversi, R., Wauthy, S., Xiao, C., Yang, J., Mosely-Thompson, E., Khodzher, T. V., Golobokova, L. P., and Ekaykin, A. A.: Ice core chemistry database: an Antarctic compilation of sodium and sulfate records spanning the past 2000 years, *Earth Syst. Sci. Data*, 15, 2517–2532, <https://doi.org/10.5194/essd-15-2517-2023>, 2023.
- Turner, J., Colwell, S. R., Marshall, G. J., Lachlan-Cope, T. A., Carleton, A. M., Jones, P. D., Lagun, V., Reid, P. A., and Iagovkina, S.: Antarctic climate change during the last 50 years, *Int. J. Climatol.*, 25, 279–294, <https://doi.org/10.1002/joc.1130>, 2005.
- Turner, J., Lu, H., White, I., King, J. C., Phillips, T., Hosking, J. S., Bracegirdle, T. J., Marshall, G. J., Mulvaney, R., and Deb, P.: Absence of 21st century warming on Antarctic Penin-

- sula consistent with natural variability, *Nature*, 535, 411–415, <https://doi.org/10.1038/nature18645>, 2016.
- Wang, Y., Thomas, E. R., Hou, S., Huai, B., Wu, S., Sun, W., Qi, S., Ding, M., and Zhang, Y.: Snow Accumulation Variability Over the West Antarctic Ice Sheet Since 1900: A Comparison of Ice Core Records With ERA-20C Reanalysis, *Geophys. Res. Lett.*, 44, 11482–411490, <https://doi.org/10.1002/2017GL075135>, 2017.
- Wille, J. D., Favier, V., Dufour, A., Gorodetskaya, I. V., Turner, J., Agosta, C., and Codron, F.: West Antarctic surface melt triggered by atmospheric rivers, *Nat. Geosci.*, 12, 911–916, <https://doi.org/10.1038/s41561-019-0460-1>, 2019.
- Zhu, J., Xie, A., Qin, X., Wang, Y., Xu, B., and Wang, Y.: An Assessment of ERA5 Reanalysis for Antarctic Near-Surface Air Temperature, *Atmosphere*, 12, 217, <https://doi.org/10.3390/atmos12020217>, 2021.